SAND2005-7704C

The Structure of Random Foam

Andrew M. Kraynik

Department 1514 MS0834, Sandia National Laboratories, Albuquerque, New Mexico 87185-0834, USA

Surface Evolver models of soap froth with a wide range of cell-size distributions are used to investigate random cellular morphology, the hallmark of foams. Geometric properties of foams and foam cells are analyzed. A simple, accurate theory relates the total surface area of foam to cell-size distribution. Total surface area is approximately equal to total edge length when both quantities are scaled by average cell volume. Voronoi structures are significantly different from foams, which raises questions over their use for predicting structure-property relationships.

Keywords: *foam structure, soap froth, Surface Evolver, surface tension, Voronoi tessellation*

1. Introduction

Random cellular morphology, the hallmark of foams [1-3], evolves when gas bubbles suspended in liquid become highly concentrated. Dispensing shaving foam and head formation on a glass of beer are familiar examples of foam production. The former involves bubble growth during foam expansion and the latter involves bubble rise and accumulation, followed by foam drainage. Producing solid foams, in general, and metal foams, in particular, also involves a phase change from liquid to solid. The films that separate gas bubbles and the Plateau borders that form along cell edges in liquid foams eventually become the cell walls and struts that are characteristic features in solid foams. Foam properties depend upon ϕ, the volume fraction of continuous phase (relative foam density), and the distribution of material in cell walls and struts; consequently when developing structure-property relationships it is important to consider the size and shape of individual cells and the way they pack together to fill space. We will investigate random cellular morphology by focusing on "dry" soap froth, an ideal but realistic model system that features well-defined local geometry shaped by surface energy minimization. In the dry foam limit where $\phi << 1$ the thin liquid films can be modeled as two-dimensional surfaces and the Plateau borders become curved lines that define cell edges. To minimize surface energy and balance mechanical forces, the local geometry satisfies Plateau's laws: 1) the faces of cells are surfaces of constant mean curvature; 2) three faces meet at equal dihedral angles of 120°; and 3) four edges meet at the tetrahedral angle 109.47°. The last condition implies that no face can be a flat polygon with straight edges when the foam is at equilibrium. Note that Plateau's laws only apply to dry soap foams where the continuous phase is well approximated by a network of surfaces.

This survey of random foam structure is based on work by Kraynik et al. [4-6], which should be consulted for additional background and details. Random foams with monodisperse, polydisperse, and bidisperse cell-volume distributions and up to 1728 cells in the representative volume (unit cell) have been simulated by using Brakke's Surface Evolver [7], the standard software for calculating the equilibrium microstructure of foam. (The software is available from: http://www.susqu.edu/facstaff/b/brakke/evolver/). All of the structures are spatially periodic, which means they fit together to fill space and represent bulk foam, especially when the number of cells is large.

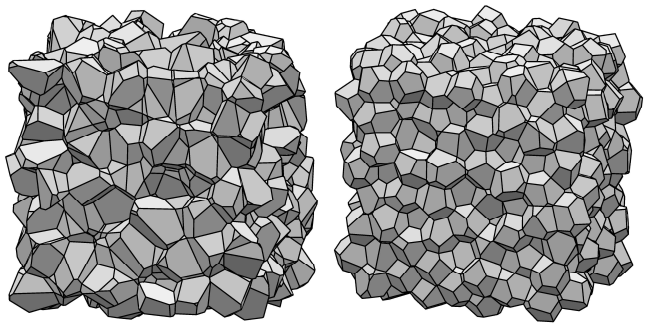

Fig. 1 Spatially periodic Voronoi tessellations with 512 cells. The structure on the left was produced from a very loose sphere packing with density $\rho = 0.01$ and the one on the right is based on random close packing where $\rho = 0.64$. The first structure is more polydisperse and has higher surface area and more faces per cell $\langle F \rangle$ than the second structure.

2. Simulations

2.1 Voronoi structures

Voronoi tessellations based on randomly distributed seed points are used as initial conditions for the Surface Evolver simulations; the seeds coincide with the centers of hard spheres that are randomly packed to density ρ. Each Voronoi cell consists of all points that lie closest to a particular seed. Voronoi structures are primitive froths with enough foam-like characteristics (three faces meet at each edge, four edges meet at each vertex, and the cells are trivalent polyhedra) that they are often used to model random foam structure. We will show that there are significant differences between Voronoi structures and foams that can affect physical properties. Voronoi polyhedra have flat faces and therefore do not satisfy Plateau's laws, which have a strong influence on the topological and geometric properties of foams and foam cells. Fig. 1 shows two Voronoi structures that were produced from different sphere packings: $\rho = 0.01$ approaches randomly distributed (Poisson) points, and at the other extreme, $\rho = 0.64$ corresponds to random close packed spheres accomplished through molecular dynamics simulations. When ρ is small the Voronoi polyhedra have highly irregular shapes with sharp angles and both the average number of faces per cell $\langle F \rangle = 15.51$ and the standard deviation of cell volumes $\sigma_V/\langle V \rangle = 0.37$ are relatively large ($\langle V \rangle$ is the average cell volume). The dense sphere packing produces Voronoi

polyhedra that are more compact and both $\langle F \rangle = 14.25$ and $\sigma_V/\langle V \rangle = 0.044$ are smaller. The latter structure also has about 7.3% less surface area and visually is more foam-like than the former.

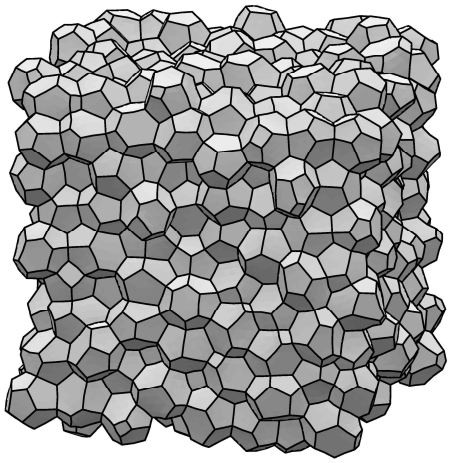

Fig. 2 Random monodisperse foam with 512 cells.

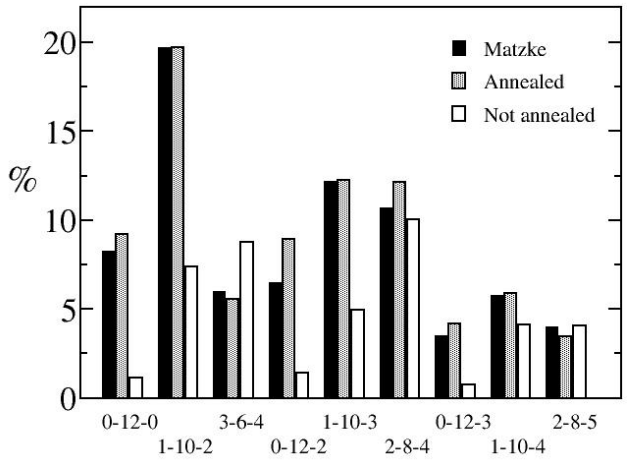

Fig. 3 Inventory (%) of the most common types of cells found in random monodisperse foam before and after annealing. The experimental data of Matzke are shown for comparison. The notation n_4-n_5-n_6 refers to cells with n_4 quadrilateral, n_5 pentagonal and n_6 hexagonal faces.

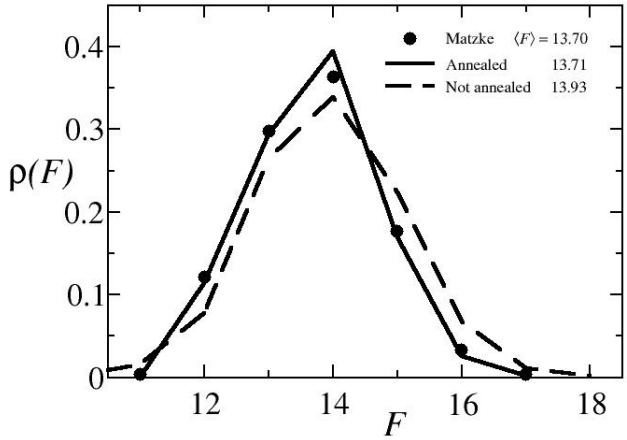

Fig. 4 The probability ρ(F) of finding cells with F faces in monodisperse foams before and after annealing.

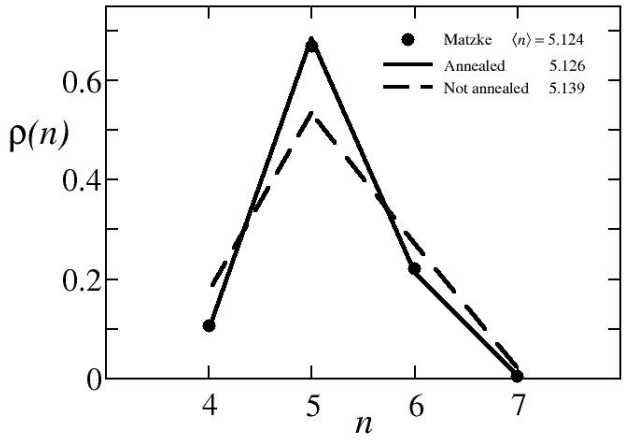

Fig. 5 The probability ρ(n) of finding faces with n edges in monodisperse foams.

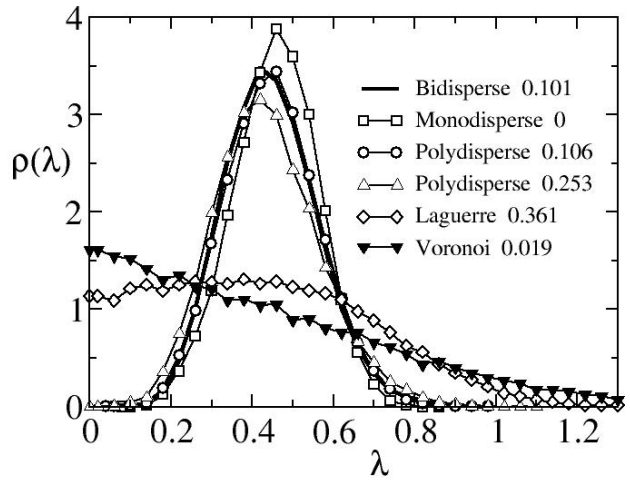

Fig. 6 The probability ρ(λ) of finding individual edges of length λ in foams with polydispersity p, as defined in Eq. (1). λ is scaled by $\langle V \rangle^{1/3}$.

2.2 Monodisperse Foam

Random monodisperse foams are produced from Voronoi structures by using the Surface Evolver to minimize surface area under the constraint that all cells have equal volume. This relaxation process requires a large number of topological transitions, which involve cell-neighbor switching, and produces faces with subtle curvatures that are required to satisfy Plateau's laws, as shown in Fig. 2. Since the solution is a local energy minimum, the surface area can be reduced even further by subjecting the foam to large-deformation tension-compression cycles that provoke additional neighbor switching; we refer to this process as annealing. Annealing has a relatively small effect on the foam energy $E = \sigma S_f$ (σ is surface tension and S_f is the total surface area per unit volume of foam) and the average number of faces per cell $\langle F \rangle$ but a significant influence on the population of cell types as classified by Matzke [8] in his classic experimental study of monodisperse foam structure; see Fig. 3. The corresponding probabilities ρ(F) that a cell has F faces and ρ(n) that a face has n edges are graphed in Figs. 4 and 5. The excellent agreement between the simulations and Matzke's data gives us a high degree of confidence that the foam structures being produced are realistic. Whereas Matzke counted and classified topological features such as faces and edges, the simulations enable us to obtain accurate data on geometric properties such as the volume, surface area, and edge length of the

entire foam, individual cells, and cell-level features. For example, Fig. 6 contains distribution functions for individual edges of length λ. The difference between foams and Voronoi structures is striking.

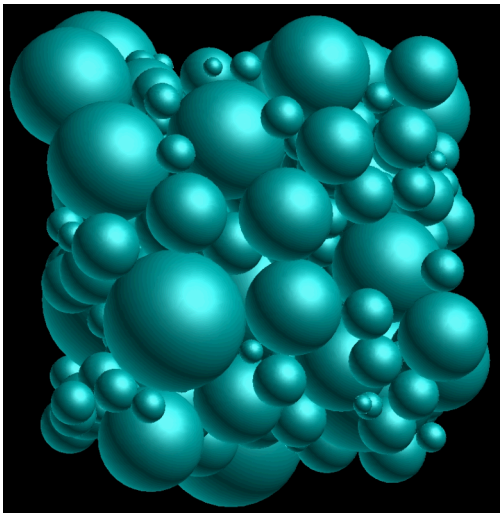

Fig. 7 This spatially periodic packing of polydisperse hard spheres was obtained by using molecular dynamics simulations.

2.3 Polydisperse Foam

The procedure for modeling random foams with a wide range of cell-size distributions starts with molecular dynamics simulations to generate dense packings of polydisperse spheres (see Fig. 7). Foam polydispersity is controlled by varying the distribution of sphere diameters (e.g., log-normal, gamma, Gaussian). Weighted-Voronoi (Laguerre) tessellations are used to fill space with convex polyhedral cells that enclose each sphere and establish the cell-size distribution. The Laguerre structure is then relaxed and annealed with the Surface Evolver to produce the foam (see Fig. 8). The cell volumes can vary by three orders of magnitude and F the number of faces on a cell ranges from four to over 150.

A useful measure of foam polydispersity p is based on the surface-volume (Sauter) mean bubble radius $R_{32} = \langle R^3\rangle/\langle R^2\rangle$:

$$p = R_{32}/\langle R^3\rangle^{1/3} - 1\,, \qquad (1)$$

where the equivalent sphere radius R is determined from $V=4\pi R^3/3$ and V is cell volume. Note that p is non-negative and equal to zero only when the foam is monodisperse. For log-normal cell-size distributions $\sigma_R/\langle R\rangle = p^{1/2}$, where σ_R is the standard deviation of R; this relation is compared with data in Fig. 9.

Figs. 10 and 11 show ρ(F) and ρ(n) for random foams with different polydispersity p. Polydisperse foams have broad distributions of F-hedra because small cells have fewer faces and large cells have more faces than monodisperse foams. As polydispersity increases we observe the following trends: the peak in ρ(F) shifts to lower F; the average face count ⟨F⟩ decreases; and the topological disorder of the foam increases (topological disorder is measured by the normalized variance of ρ(F): $\mu_2/\langle F\rangle^2 = \langle F^2\rangle/\langle F\rangle^2 - 1$). Compared to ρ(F) the distribution of n-gons measured by ρ(n) is less sensitive to polydispersity, especially when p is small. Pentagonal faces are most abundant unless the foam is extremely polydisperse. The relationship between various statistical quantities is shown in Fig. 9. In contrast with the Voronoi structures pictured in Fig. 1, the average number of faces in relaxed foams is less than fourteen and ⟨F⟩ decreases as p increases.

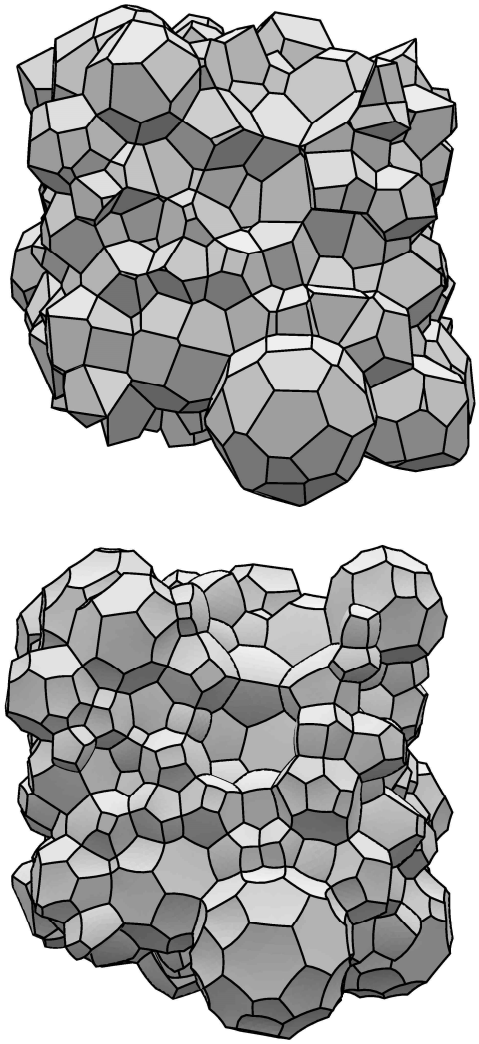

Fig. 8 The weighted-Voronoi (Laguerre) tessellation (top) is relaxed to obtain the polydisperse foam (bottom).

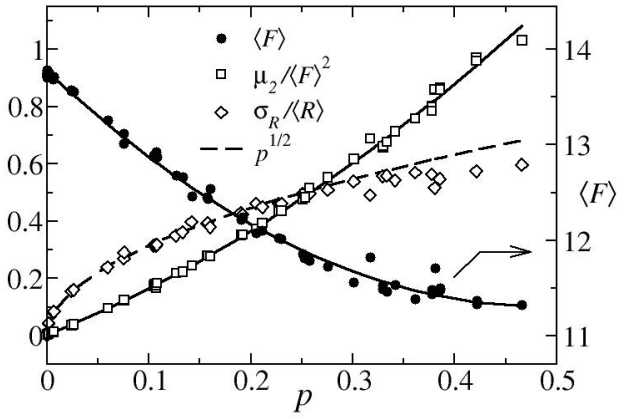

Fig. 9 The average face count ⟨F⟩, topological disorder $\mu_2/\langle F\rangle^2$, and an alternate measure of polydispersity $\sigma_R/\langle R\rangle$ are graphed against polydispersity p. The solid lines are quadratic fits to guide the eye and the dashed line is $p^{1/2}$.

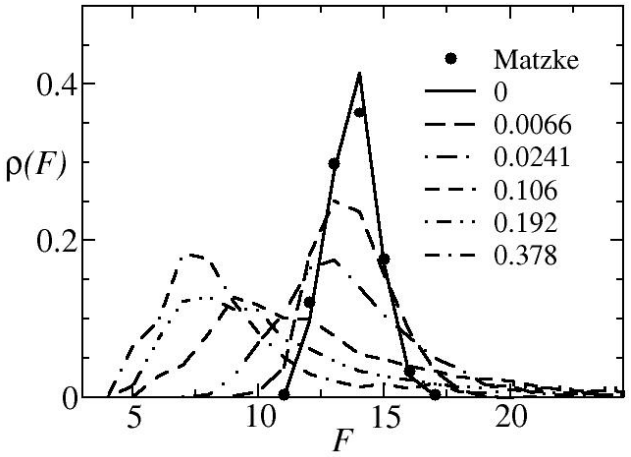

Fig. 10 Distribution of cells with F faces in foams with different polydispersity p.

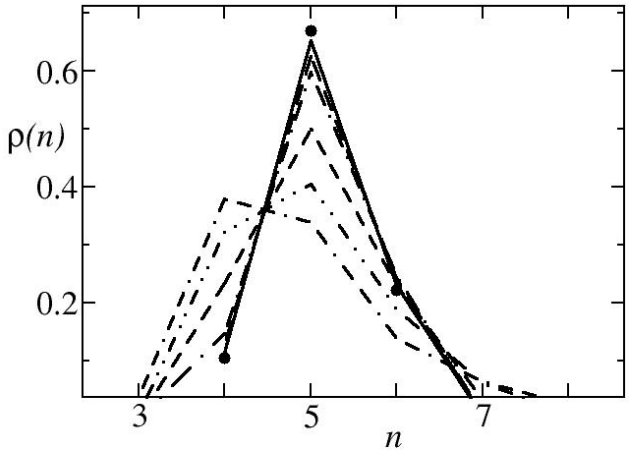

Fig. 11 Distribution of faces with n edges in foams with different polydispersity p. (Same legend as Fig. 10.)

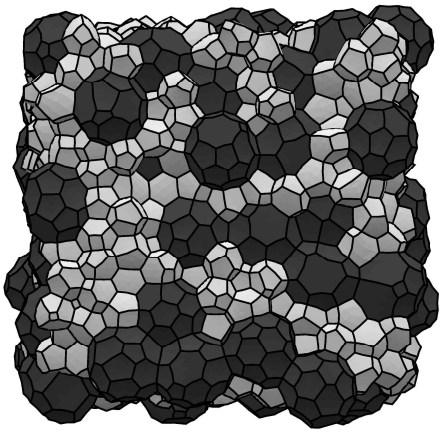

Fig. 12 Bidisperse foam with 1000 cells, $V_L/V_S = 8$ and faction of large cells $X_L = 1/9$.

2.4 Bidisperse foam

Bidisperse foams are produced from bidisperse sphere packings by constraining the cells to have two different volumes, as shown in Fig. 12. The simulations are in good agreement with topological statistics obtained by Matzke and Nestler [9] on foams with cell-volume ratio $V_L/V_S = 8$ and three different fractions of large cells.

2.5 Geometric properties

The simulations enable us to gather a wide variety of geometric statistics. The most striking result involves the surface area S of individual cells, which is found to be about 10% greater than a sphere of equal volume. The reduced surface-to-volume ratio $\beta = S/(36\pi V^2)^{1/3}$ is graphed against F in Fig. 13; β is very insensitive to F and has a very narrow range: $\beta = 1.100 \pm 0.008$. This is a consequence of Plateau's laws, as illustrated by the foam cells pictured in Fig. 14: the faces on cells with small F curve outward, reducing β relative to the flat-faced Laguerre polyhedra; and the faces on cells with large F curve inward, increasing β just like the "dimples" on a golf ball.

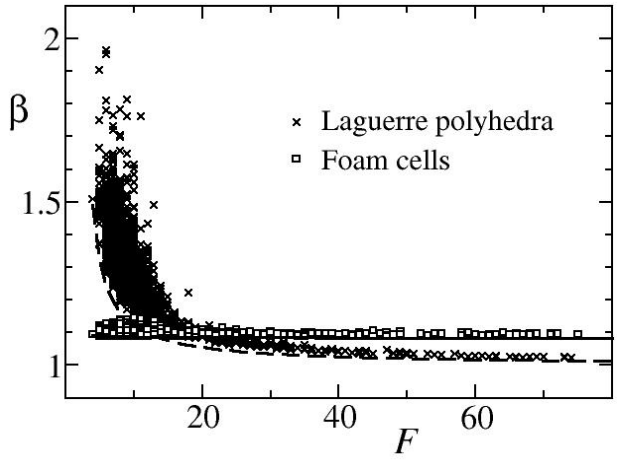

Fig. 13 Reduced surface-to-volume ratio β of foam cells and Laguerre polyhedra graphed against the number of faces F and compared with the theory for isotropic Plateau polyhedra (IPP, solid line) and convex isotropic polyhedra (CIP, dashed line).

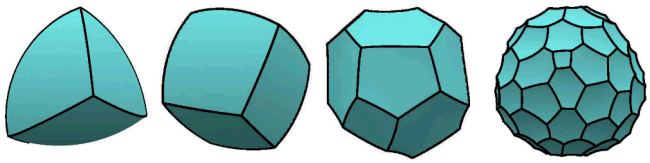

Fig. 14 Shape of typical foam cells with four, six, 14 and 60 faces.

By assuming that β is constant, we can derive a very simple theory for the surface free energy density of foam:

$$E = \sigma S_f = \beta (36\pi)^{1/3} (1+p)^{-1} \sigma \langle V \rangle^{-1/3}, \qquad (2)$$

where σ is surface tension and S_f is the total surface area per unit volume of foam. The results in Fig. 15 show that the theory is in excellent agreement with simulations for foams that have a wide range of cell-size distributions and have been annealed. This indicates that the foam energy or total surface area can be calculated very accurately by knowing the cell-size distribution. We have also found that the total edge length per unit volume of foam L_f is approximately equal to the total surface area S_f when both quantities are normalized by the average cell volume. The data in Fig. 16 support the empirical relationship: $L_f \langle V \rangle^{2/3} \approx S_f \langle V \rangle^{1/3}$. Some of the scatter in the data can be attributed to weak dependence on the shape of the cell-size distribution [10].

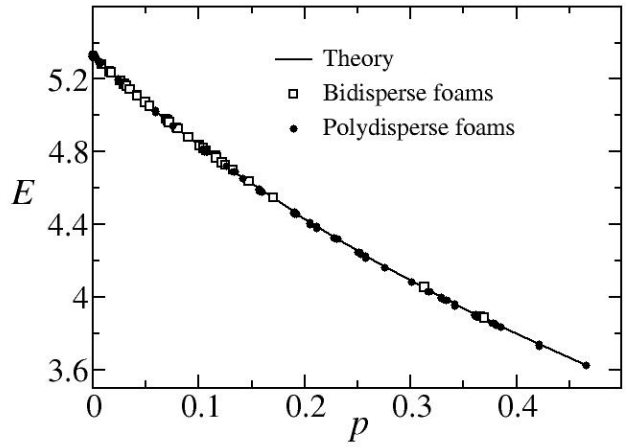

Fig. 15 Foam energy E (or normalized surface area $S_f \langle V \rangle^{1/3}$) plotted against polydispersity p and compared with the theory in Eq. (2) with $\beta = 1.10$. Energy is scaled by $\sigma \langle V \rangle^{-1/3}$.

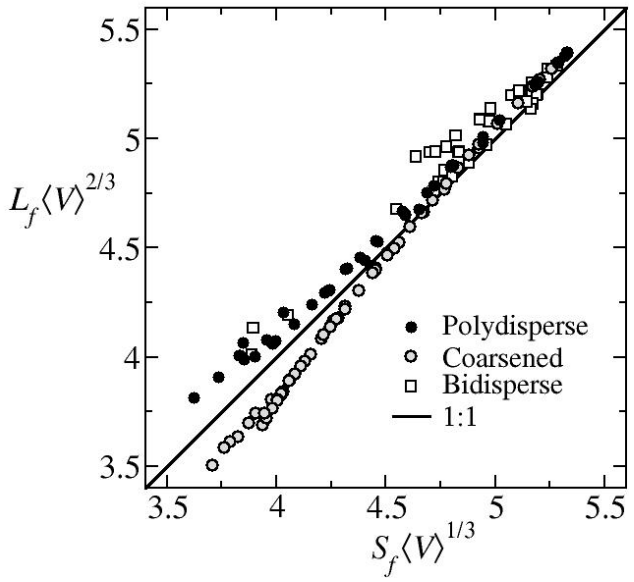

Fig. 16 The normalized edge length of a foam $L_f \langle V \rangle^{2/3}$ is approximately equal to the normalized surface area $S_f \langle V \rangle^{1/3}$.

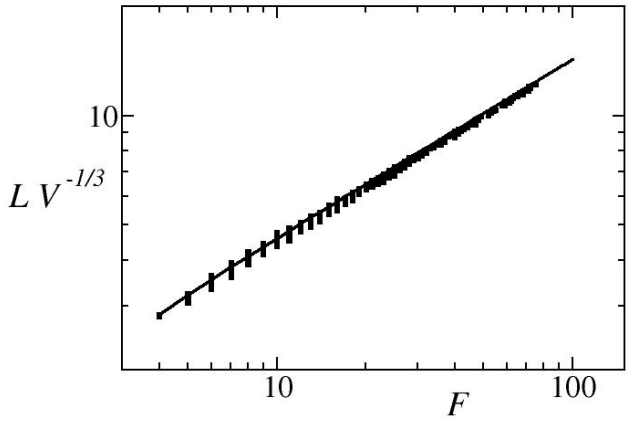

Fig. 17 Total edge length L of individual cells is graphed against number of faces F; simulations are compared with IPP theory.

Other geometric properties of foam cells such as the total edge length L and the average mean curvature of the faces both depend on cell topology as measured by F. This dependence is captured by the theory of idealized foam cells called isotropic Plateau polyhedra [11] (IPP), which have F identical spherical-cap faces and satisfy Plateau's laws. Convex isotropic polyhedra (CIP) are flat-faced counterparts of IPP. The predictions of IPP and CIP theory for β are shown in Fig. 13; neither theory contains adjustable constants. Fig. 17 shows a comparison between L from simulations and IPP theory, which predicts $F^{1/2}$ dependence.

The average curvature of the faces can be expressed as the dimensionless diffusive growth rate *G* given by

$$G = V^{-1/3} \int \mathcal{H} \, da \,, \qquad (3)$$

where $\mathcal{H}$ is the mean curvature and the integral is evaluated over the cell surface. Fig. 18 compares data for *G* with IPP theory.

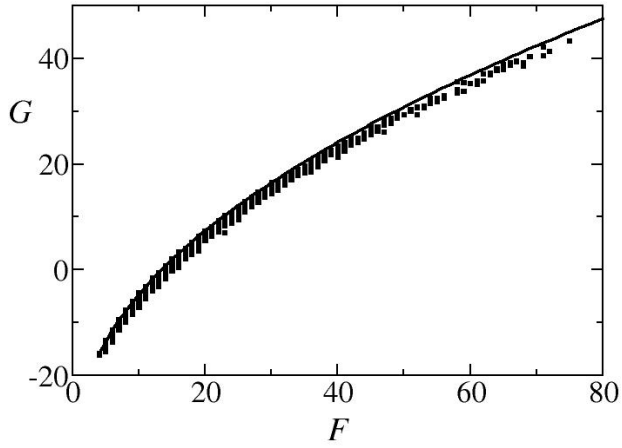

Fig. 18 Diffusive growth *G* of individual cells is graphed against number of faces F; simulations are compared with IPP theory.

Fig. 6 also contains the edge-length distribution ρ(λ) for a weighted-Voronoi structure and polydisperse and bidisperse foams. Voronoi structures that are based on random seeds have many small edges. In sharp contrast, ρ(λ) has Gaussian character for all of the relaxed foams. The difference is dramatic and raises caution against using Voronoi structures to model real foams, especially when the foam property of interest is sensitive to edge-length characteristics.

3. Wet Foams

The Surface Evolver [7] can be used to model wet foams in the dry-film limit where all of the liquid is assumed to be located in the Plateau borders because the film thickness set by colloidal forces is so small. These calculations demand much more computational effort than dry foams because of the large number of facets required to discretize the Plateau borders. Fig. 19 shows unit cells for two structures: the wet Kelvin foam and the wet rhombic dodecahedral foam, which are associated with body-centered-cubic and face-centered-cubic lattices, respectively. Both of these structures are stable over some overlapping range of liquid volume fraction, which indicates that there are two perfectly ordered wet foams, whereas the Kelvin cell is the only perfectly ordered dry foam. Eight Plateau borders meet at some of the junctions in the wet dodecahedron; this is permitted since Plateau's laws do not apply to foams with finite liquid content.

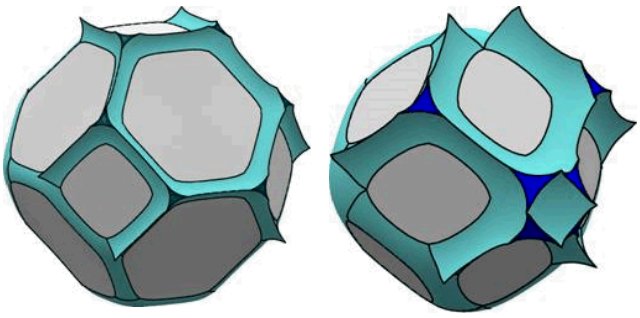

Fig. 19 The wet Kelvin cell (left) has liquid volume fraction $\phi = 0.01$ and the wet rhombic dodecahedron (right) has $\phi = 0.04$.

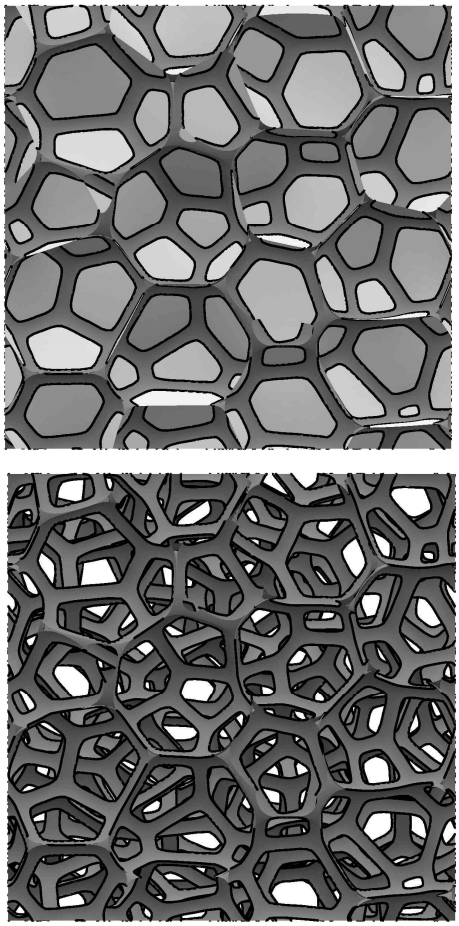

Fig. 20 Random monodisperse wet foam with 64 cells and $\phi = 0.025$. The films have been removed in the lower image to reveal the network of Plateau borders.

Fig. 20 shows the unit cell of a wet random monodisperse foam with 64 cells and $\phi = 0.025$. When the films are removed the wet foam looks like a solid foam with open cells; this suggests that wet foams may provide useful models for the strut-level geometry of open-cell foams. The figure reveals the variation in cross-section along individual "struts" that is a characteristic feature of open-cell foams. As an example of the microstructural information that can be obtained from simulations, Fig. 21 shows the dependence of strut cross-section on strut length. The radius of curvature R_{PB} is evaluated from the cross-sectional area at the center of each strut by assuming ideal Plateau-border shape, the curved triangular region defined by three circles in mutual contact. This information can be used to develop a model for strut shape, which in turn can be used to build realistic beam element models for open-cell foams that are based on soap-froth microstructure, as shown in Fig. 22. Spatial periodicity is beneficial because many foam micromechanics problems are very sensitive to boundary conditions.

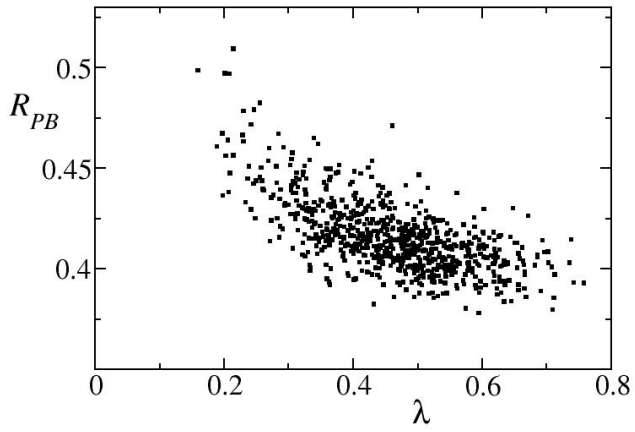

Fig. 21 Minimum strut cross-section R_{PB} vs. strut length λ evaluated from the random wet foam structure shown in Fig. 20.

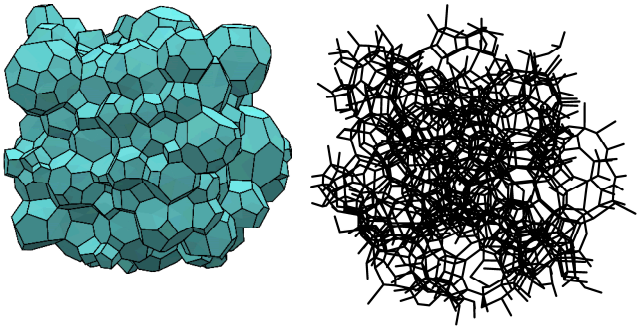

Fig. 22 The random polydisperse soap froth was used as a template to create a beam model of a low-density open-cell foam.

Sandia is a multiprogram laboratory operated by Sandia Corporation, a Lockheed Martin Company, for the United States Department of Energy's National Nuclear Security Administration under contract DE-AC04-94AL85000.

REFERENCES

1) L. J. Gibson and M. F. Ashby: *Cellular Solids: Structure and Properties* 2nd Ed. (Cambridge University Press, Cambridge, England, 1997)
2) D. Weaire and S. Hutzler: *The Physics of Foams*, (Oxford University Press, Oxford, 1999).
3) M. F. Ashby, A. Evans, N. A. Fleck, L. J. Gibson, J. W. Hutchinson and H. N. G. Wadley: *Metal Foams: A Design Guide*, ((Butterworth-Heinemann, Boston, 2000).
4) A. M. Kraynik, D. A. Reinelt and F. van Swol, Phys. Rev. E **67** (2003) 031403.
5) A. M. Kraynik, D. A. Reinelt and F. van Swol, Phys. Rev. Lett. **93** (2004) 208301.
6) A. M. Kraynik, D. A. Reinelt and F. van Swol, Coll. Surf. A **263** (2005) 11-17.
7) K. A. Brakke: Experimental Mathematics **1** (1992) 141-165. http://www.susqu.edu/facstaff/b/brakke/evolver/
8) E. B. Matzke: Am. J. Botany **33** (1946) 58-80.
9) E. B. Matzke and J. Nestler: Am. J. Botany **33** (1946) 130-144.
10) D. A. Reinelt and A. M. Kraynik: Phys. Rev. E Submitted.
11) S. Hilgenfeldt, A. M. Kraynik, D. A. Reinelt and J. M. Sullivan: Europhys. Lett. **67** (2004) 484-490.